

# Joint probability analysis of storm surge and wave caused by tropical cyclone for the estimation of protection standard: a case study on the eastern coast of the Leizhou Peninsula and Hainan Island of China

Zhang Haixia<sup>1,2,3,4</sup>, Cheng Meng<sup>1,2,3,4</sup>, Fang Weihua<sup>1,2,3,4</sup>

<sup>1</sup> Key Laboratory of Environmental Change and Natural Disasters, Ministry of Education, Beijing Normal University, 100875, Beijing, China

<sup>2</sup> Academy of Disaster Risk Science, Faculty of Geographical Science, Beijing Normal University, 100875, Beijing, China

<sup>3</sup> Southern Marine Science and Engineering Guangdong Laboratory (Guangzhou), 511458, Guangzhou, Guangdong, China

<sup>4</sup> State Key Laboratory of Earth Surface Processes and Resource Ecology (ESPRE), Beijing Normal University, 100875, Beijing, China

Correspondence to: Weihua Fang (weihua.fang@bnu.edu.cn)

**Abstract.** [The impact of natural hazards such as storm surges and waves on coastal areas during extreme tropical storm events can be amplified by the cascading effects of multiple hazards. Quantitative estimation of the marginal distribution and joint probability distribution of storm surge and wave is essential to understanding and managing tropical cyclone disaster risks. In this study, the dependence between storm surges and waves is quantitatively assessed using the extreme value theory and copula function for the Leizhou Peninsula and Hainan Island of China, based on the numerically simulated surge height \(SH\) and significant wave heights \(SWH\) for every 30 minutes from 1949 to 2013. The steps for determining coastal protection standards in scalar values are also demonstrated. It is found that, first, the generalized extreme value \(GEV\) function and Gumbel copula function are suitable, respectively, for fitting the marginal and joint distribution characteristics of the SHs and SWHs in this study area. Additionally, SH shows higher values as locations get closer to the coastline, and SWH becomes higher further from the coastline. Lastly, the optimal design criteria of SH and SWH under different joint return periods can be estimated using the non-linear programming method. This study shows the effectiveness of the bivariate copula function in evaluating the probability for different scenarios, providing a valuable reference for optimizing engineering design criteria.](#)

**Keywords:** Joint probability analysis, Storm surge and wave, Copula function, Tropical cyclone, Leizhou Peninsula and Hainan Island

删除了: Quantitatively estimating combined storm surge and wave hazards provides scientific guidance for disaster prevention, mitigation, and relief in coastal cities. The marginal and copula functions are preferred based on the Kolmogorov-Smirnov test pass rate, and the relationship between storm surge and wave is quantitatively evaluated using the optimal function, then the bivariate risk probabilities are estimated....

删除了: The results show that

删除了: surge height and significant wave height

删除了: , respectively

删除了: Second

删除了: the surge height

删除了: an increasing trend

删除了: the significant wave height

删除了: is

删除了: Third

删除了: when one variable is constant, the simultaneous, joint, and conditional risk probability tends to decrease as the other variable increases. In actual engineering design, improving the protection standard can effectively reduce the bivariate risk probability. In addition, we can estimate the optimal design criteria for different joint return periods by the

删除了: that

删除了: the

删除了: can effectively evaluate

删除了: risk

删除了: which

删除了: provides

删除了: engineering

删除了: protection standards

## 1 Introduction

65 [Tropical cyclone storm surges and waves could cause severe loss of life and property in offshore and coastal areas \(Chen and Yu, 2017; Marcos et al., 2019; Wahl et al., 2015\)](#), and it is of great importance to quantify the intensity-frequency relationship of storm surges and waves, to understand the joint severity of multi-hazard extreme tropical cyclones (Zhang and Wang, 2021; Galiatsatou and Prinos, 2016).

In the past, many studies have analyzed the single hazard indicators for tropical cyclone storm surges and waves (Lin et al., 2010; Shi et al., 2020; Teena et al., 2012), often with observed time series data, or with or simulated results by numerical models (Petroliagkis et al., 2016; Bilskie1 et al., 2016; Huang et al., 2013; Papadimitriou et al., 2020). [The intensity values of the surge height \(SH\) or significant wave height \(SWH\) of a specific return period can be estimated based on extreme value theory \(Teena et al., 2012; Muraleedharan et al., 2007; Morellato and Benoit, 2010; Niedoroda et al., 2010\)](#). Accordingly, the estimated probabilities of single hazards, such as SH or SWH, have also been widely applied in the protection standard design in coastal areas (Bomers et al., 2019; Perk et al., 2019; Lee and Jun, 2006).

75 However, strong storm surges and waves often occur simultaneously during tropical cyclone events, which often cause greater impact than estimated only by a single variate due to the cascading effects of multi-hazards. For example, when high waves near the coast take place along strong storm surges, the overtopping and overflowing at sea dyke can lead to a large area of inundation and severe damage to coastal facilities (Rao et al., 2012; Hughes and Nadal, 2009; Pan et al., 2019). Similarly, rising sea levels due to storm surges would improve the probability of wave overtopping (Pan et al., 2013; Li et al., 2012). The concurrent interaction between storm surges and waves often assesses the effects of multi-hazards with significant uncertainties. Some studies have investigated the physical interaction of storm surges and waves through numerical simulation by coupling storm surge and wave models (Xie et al., 2016; Kimf et al., 2016; Brown, 2010) for specific events.

85 Statistical tools such as joint probability analysis have been used in multidimensional natural hazard assessment (Hsu et al., 2018). Since the Copula function does not restrict the marginal distribution function and can be relatively easily extended to multiple dimensions, it is often used to construct joint probability of multiple variates (Nelsen, 2006; Chen and Guo, 2019). There are a variety of applications with Copula function for double hazards, for example, rainfall and storm surge (Jang and Chang, 2022), wind and storm surge (Trepanier et al., 2015), and storm surge and wave (Corbella and Stretch, 2013; Wahl et

al., 2012).

In coastal protection standard design, it is essential to analyze and estimate the joint probability of SH and SWH. Chen et al. (2019) used the copula functions to analyze the joint probability of extreme wave height and surge height at nine representative stations along China's coasts. Galiatsiou and Prinos (2016) investigated the joint probability of extreme wave heights and storm surges with time by a non-stationary bivariate approach. Marcos et al. (2019) statistically assessed the dependence between extreme storm surges and wind waves along global coastal areas using the outputs of numerical models. Most previous joint probability studies on storm surges and waves mainly focused on location-specific rather than region-wide analysis. In addition, even with the joint probability of bivariate estimation, only an intercepted curve can be obtained since their probability is a three-dimensional surface. It is not applicable for actual protection design without a specific scalar value for SH or SWH.

In this study, we aim to explore the joint probability characteristics of tropical cyclone storm surges and waves for large coastal areas and to investigate the methods and steps for selecting the protection standard of sea dikes. Firstly, we fit the marginal and copula function of nodes in the study area based on the numerically simulated tropical cyclone SH and SWH from 1949 to 2013. Next, the optimal functions are selected for every modeling node based on the Kolmogorov-Smirnov (K-S) test, AIC, and BIC. Then, the correlation between SH and SWH is quantified using the copula function to calculate the probabilities under simultaneous, joint, conditional, and different-level combinations. Finally, the bivariate probability changes caused by increasing SH and SWH are quantitatively assessed, and the design storm surges and waves for different joint return periods are estimated based on a non-linear programming method.

## 2. Study area and data

### 2.1 Best tracks of TCs

The best track dataset of historical TCs in the Northwest Pacific (NWP) is obtained from the Tropical Cyclone Data Center of the China Meteorological Administration (CMA). The CMA records in detail the location (longitude and latitude), time (year, month, day, hour), central minimum pressure, and 2-minute average near-center maximum sustained wind speed (MSW) for

删除了: In the background of rising sea surface temperatures (SSTs), the lifetime of tropical cyclones (TCs) is extended and their intensity is enhanced. In particular, the frequency of severe tropical storms (STSs) and storms with higher intensity levels has significantly increased (Emanuel, 2005; Elsner et al., 2008; Sun et al., 2017), triggering more tremendous storm surges and wave disasters and causing severe casualties and property damage in offshore and coastal areas (Chen and Yu, 2017). Accurate and rapid assessment of tropical cyclone storm surge and wave occurrence probability and intensity is essential for actively and effectively preventing extreme disaster risks (Zhang and Wang, 2021; Teena et al., 2012).

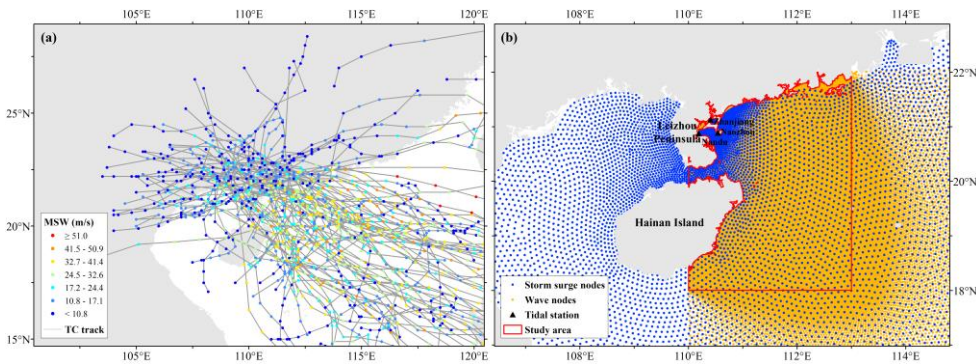
删除了: Tropical cyclone storm surges and waves significantly threaten marine fishing, aquaculture, marine transportation, offshore oil and gas development, and other offshore production activities (Jin et al., 2018; Guo et al., 2020). When storm surges are accompanied by waves near the coast, they cause severe damage to coastal dikes, breakwaters, revetments, industrial facilities, roads, and bridges (Rao et al., 2012; Hughes and Nadal, 2009). When the sea level in front of the sea dike caused by a superstorm surge exceeds the top of the sea dike or when gales and waves cause damage to the wave wall at the top of the sea dike, it can cause the sea dike to suffer from both overtopping waves and overflowing surges (Pan et al., 2013, 2019; Li et al., ...)

删除了: <#>Study area

Based on the location of the nodes of the triangular network in the storm surge (Section 2.3) and wave datasets (Section 2.4), we select the region with a dense distribution of both as the study area, and the finalized spatial range is 110°E - 113°E, 18°N - 22°N (Figure 1b). This area is east of the Leizhou Peninsula and Hainan Island in the South China Sea, which is also the area most frequently affected by tropical cyclones in China. Based on the dataset of surge height (S<sub>TD</sub> ...)

删除了: , UTC

205 every 6-hour track point of each TC event since 1949 (Lu et al., 2021). The landfall of TCs in China is concentrated on the southeast coast, especially in the coastal areas of the South China Sea. Figure 1a shows the spatial distribution of the best track and maximum sustained wind speed of 86 historical TCs screened in this study from 1949 to 2013.



210 **Figure 1: Best track and MSW of 86 TCs in this study from 1949 to 2013 (a) and the study area for the joint probability analysis of storm surges and waves of TCs (b).**

## 2.2 Surge heights

215 The TC surge heights (SHs) dataset is obtained from the Ocean University of China, mainly through the Advanced CIRCulation model (ADCIRC) simulations, which includes the SHs of 86 TCs affecting the eastern coast of the Leizhou Peninsula and Hainan Island from 1949 to 2013 (Liu et al., 2018; Li et al., 2016). The previous study provides a water depth map for the study area (Liu et al., 2018). The ADCIRC model integrates the effects of various boundary conditions and external forcing and uses triangular grids with different resolutions, making it more computationally efficient and applicable in numerical simulations. The simulation results are the total water level after the superposition of the water gain caused by a tropical cyclone and astronomical tide, and the time step is 30 minutes. To improve the simulation accuracy and computing speed of the hot spot area, the model adopts a triangular grid with nested small- and large-area grids, and the resolutions of different area grids are set in a gradual resolution range from 0.0039° to 0.3°. Comparing the simulation values with the measured surge height at the observation sites, we discover that the absolute standard error is 47 cm, the relative standard error is 22%, and the simulation results are similar to the observed values in most cases. Thus, the dataset could be used to assess

删除了: are derived from

删除了: Advanced

删除了: Circulation

删除了: Model

删除了: simulation results

删除了: 119

删除了: of the simulation

删除了: network

删除了: that

the hazard of TC storm surges. Figure 2a shows an example of the simulation results of the surge height of TC *Nasha* (ID:1117) at a specific moment.

### 2.3 Significant wave heights

The TC significant wave heights (SWHs) dataset is also obtained from the Ocean University of China, mainly through the Simulating WAVes Nearshore (SWAN) model, and includes the SWHs of 86 TC events affecting the study area from 1949 to 2013 (Li et al., 2016). The SWAN model has the advantage of high computational accuracy and stability and has been widely used in numerical simulations of offshore waters. The simulation results include indicators such as significant wave height, mean period, and wave direction, and the time step is 1 hour. The model also uses a triangular grid with nested small- and large-area grids and gradual resolution, but the nodes' scopes and locations differ from those of the storm surge model. Comparing the observed data of buoy stations with the simulated values reveals that the unstructured grid can well reflect the wave variation conditions in the sea. In addition, the mean absolute and root mean square errors of the simulated results of the locally encrypted unstructured triangular grid are the smallest, indicating that the data can effectively reproduce the wave distribution during tropical cyclones. It shall be noted that the effect of sea level rise due to storm surge was not considered during the SWH simulation, which will influence the accuracy of SWHs, especially in intermedia and shallow water. In this paper, we choose the SWH as an indicator of tropical cyclone wave hazard. Figure 2b shows an example of the significant wave height of TC *Nasha* (ID: 1170) at a specific moment.

- 删除了: are simulated using
- 删除了: including
- 删除了: 102
- 删除了: Leizhou Peninsula
- 删除了: 2014
- 删除了: simulation
- 删除了: network
- 删除了: A comparison of
- 删除了: error and root mean square error
- 删除了: network
- 删除了: mainly
- 删除了: s

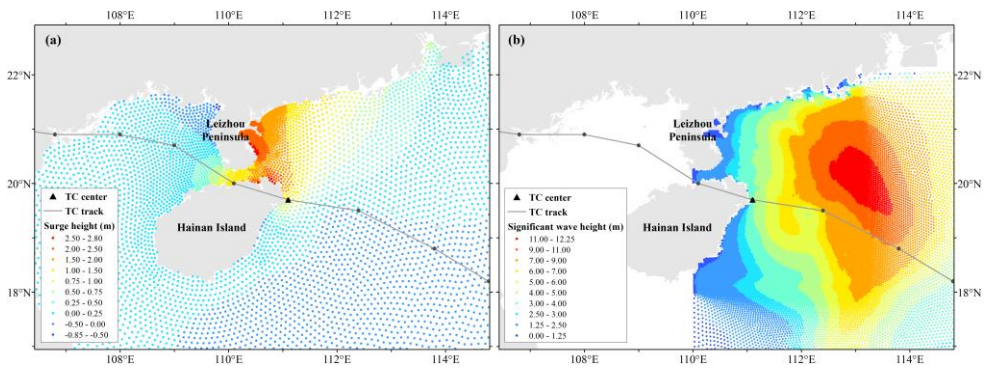


Figure 2: Distribution of surge height (a) and significant wave height (b) at a specific moment of TC Nasha (ID: 1117) (UTC: 2011.9.29 6:00:00)

## 2.4 Study area

Based on the location of the nodes of the triangular grid in the storm surge (Section 2.2) and wave datasets (Section 2.3), we select the region with a dense distribution of both as the study area, and the finalized spatial range is 110°E - 113°E, 18°N - 22°N (Figure 1b). This area is located east of the Leizhou Peninsula and Hainan Island in the South China Sea, which is one of the most frequently affected areas by tropical cyclones in China. Based on the dataset of surge height (SH) and significant wave height (SWH) of tropical cyclones, we screen 86 historical tropical cyclones (TC) events that simultaneously affected the study area from 1949 to 2013 for joint probability characteristics analysis of storm surge and wave.

## 3 Methods

Sklar (Sklar, 1973) elucidates the role that copula play in the relationship between multivariate distribution and their univariate margins distribution, and states that any multivariate joint distribution can be described by a univariate marginal distribution function and a couple describing the dependence structure between the variables (Nelsen, 2006). Let  $F(x)$  and  $G(y)$  be the marginal distributions of  $x$  and  $y$ ,  $C$  is the copula, and  $H(x, y) = C(F(x), G(y))$ , where  $H$  is the bivariate joint distribution function of  $x$  and  $y$  (Serinaldi, 2015). Therefore, the copula function is widely utilized in multi-hazard joint probability analysis of natural disasters (Chen et al., 2019; Lee et al., 2013).

### 3.1 Marginal function

The marginal function means that the probability density function (PDF) and cumulative distribution function (CDF) of the univariate are constructed by intensity-frequency analysis to reflect the probability of occurrence of the univariate at different intensities. The method is widely utilized in natural hazard assessments such as tropical cyclones, floods, droughts, and earthquakes. We select five commonly employed marginal functions for the annual extreme values fitting of tropical cyclone storm surges and waves, including the Gumbel, Weibull, gamma, exponential, and generalized extreme value (GEV) functions. In this study, the maximum likelihood method is used to estimate the function parameters, based on which the optimal marginal

删除了: proposed that any multivariate joint distribution can be composed of multiple univariate marginal distribution functions and a copula function describing the correlation structure among various variables, i.e., Sklar's theorem, which is the basis of copula theory and applications. Therefore, the copula function refers to the role that connects the marginal distribution functions and is also known as the link function, which can accurately calculate the risk probability with the combination of multivariate encounters according to the actual situation and is widely utilized in the joint probability analysis of multihazard indicators in natural disasters...

删除了: distribution

删除了: distribution

删除了: fitting

删除了: likelihood

删除了: the

删除了: This paper

删除了: s

删除了: distribution

删除了: distributions

functions for SHs and SWHs are screened by the following steps: Firstly, the p-value of the K-S test is used to determine whether each node rejects the hypothesis that the samples obey a certain functional distribution. Secondly, the optimal function for each node is screened by the three metrics, AIC, BIC, and D-value of the K-S test. The smaller the AIC, BIC, and D-value of the K-S test, the better the goodness of fit, thus determining the optimal marginal function for each node. Finally, an optimal function is selected as the univariate marginal function for all nodes, and its PDF and CDF are fitted.

删除了: Next, we use the maximum likelihood method to estimate the fitting parameters, based on which we determine the goodness of fit of each node by the Kolmogorov–Smirnov (K-S) test. An...

删除了: distribution

### 3.2 Bivariate copula function

There are a variety of copulas families, including Meta-elliptical copulas (normal and t), Archimedean copulas (Clayton, Gumbel, Frank, and Ali-Mikhail-Haq), Extreme Value copulas (Gumbel, Husler-Reiss, Galambos, Tawn, and t-EV), and the other families (Plackett and Farlie-Gumbel-Morgenstern) (Chen and Guo, 2019). Among these copulas, the Archimedean copula is more popular for hydrologic applications. The commonly employed Archimedean copula functions include Gumbel, Clayton, and Frank (Table 1), which are selected to analyze the joint probabilities of two variables, the SHs, and SWHs of a tropical cyclone. Then the maximum likelihood method is used to estimate the parameters of the copula function. Next, we fit the goodness-of-fit of copula functions for the tropical cyclone storm surge and waves at each node by the K-S test. According to the passing rate of the K-S test at the sample nodes, an optimal function is selected as the copula function for all nodes of the two-dimensional variables, and the PDF and CDF are calculated.

删除了: Table 1 Table 1

设置了格式: 字体颜色: 文字 1

删除了: There are three families of copula functions: elliptical, Archimedean, and quadratic. Archimedean copula functions are simple to construct and contain only one parameter, which is convenient for solving and has been widely used in hydrological multivariate frequency calculations. The commonly employed Archimedean copula includes Gumbel, Clayton, and Frank (Table 1), which are chosen in this paper to analyze the joint probabilities of the marginal distributions of two variables, tropical cyclone storm surge and waves, and to estimate the parameters of the copula function using the maximum likelihood method.

删除了: bivariate

删除了: points

删除了: of the two-dimensional variables

**Table 1 Formulas and parameter ranges for three types of bivariate Archimedean copula functions.**

Name of copula	Bivariate Copula	Parameter $\theta$
Clayton	$C_{\theta}(u, v) = [\max\{u^{-\theta} + v^{-\theta} - 1, 0\}]^{-1/\theta}$	$\theta \in [-1, \infty) \setminus \{0\}$
Frank	$C_{\theta}(u, v) = -\frac{1}{\theta} \log \left[ 1 + \frac{(e^{-\theta u} - 1)(e^{-\theta v} - 1)}{e^{-\theta} - 1} \right]$	$\theta \in \mathbb{R} \setminus \{0\}$
Gumbel	$C_{\theta}(u, v) = \exp \left[ -\left( (-\log(u))^{\theta} + (-\log(v))^{\theta} \right)^{\frac{1}{\theta}} \right]$	$\theta \in [1, \infty)$

Note:  $u$  and  $v$  are uniform (0,1) random variables (Nelsen, 2006).

### 3.3 Joint probability of storm surges and waves

#### 3.3.1 Univariate return period

The return period (RP) indicates the period of natural hazard events, and it is a crucial indicator for quantifying the hazard level, which is widely utilized in hazard analysis. The formula for the return period of a single hazard indicator is as follows.

$$RP_X = \frac{E_L}{1 - F_X(x)} = \frac{E_L}{1 - P(X \leq x)} \quad (1)$$

where  $RP_X$  is the return period of the univariate  $X$ ;  $F_X(x) = P(X \leq x)$  is the marginal function of the univariate  $X$ , and  $E_L$  denotes the time interval of the sample series of the univariate  $X$ , the value is taken as 1 in this paper.

#### 3.3.2 Bivariate probability and return period

Based on the copula function, it can quantitatively estimate the probability of a multivariate being greater than a specified threshold. The bivariate probability refers to the likelihood that various conditions will occur simultaneously, and the bivariate return period refers to the average time interval required for multiple states to be simultaneously greater than a certain threshold.

The definitions of three types of joint probabilities and return periods are given according to the univariate return period formula. The first type is when two variables simultaneously reach a given threshold, which will be defined as the simultaneous probability  $P_0$  (Eq. 2) and simultaneous return period  $RP_0$  (Eq. 3). The second type is that at least one variable reaches a given threshold, which is defined as the joint probability  $P_U$  (Eq. 4) and joint return period  $RP_U$  (Eq. 5). The third type is the conditional probability  $P_1$  (Eq. 6) and conditional return period  $RP_1$  (Eq. 7), where when one of the variables reaches a given threshold, the other variable also reaches a certain threshold. The formula is as follows (Serinaldi, 2015):

$$P_0 = P((X > x) \cap (Y > y)) = 1 - P(X \leq x) - P(Y \leq y) + P(X \leq x, Y \leq y) \\ = 1 - F_X(x) - F_Y(y) + F_{X,Y}(x, y)$$

$$RP_0 = \frac{E_L}{P((X > x) \cap (Y > y))} = \frac{E_L}{1 - F_X(x) - F_Y(y) + F_{X,Y}(x, y)}$$

$$P_U = P((X > x) \cup (Y > y)) = 1 - P(X \leq x, Y \leq y) = 1 - F_{X,Y}(x, y)$$

$$RP_U = \frac{E_L}{P((X > x) \cup (Y > y))} = \frac{E_L}{1 - F_{X,Y}(x, y)}$$

删除了: ;...and it is a crucial indicator for quantifying the hazard level, which is widely utilized in disaster ...azardrisk...analysis. The formula for the return period of a single hazard indicator is disaster-causing factor  $\frac{RP}{E_L}$

删除了: expressed

删除了: 112

删除了: distribution

删除了: ,

删除了: ...theThe

删除了: risk

删除了: multiple variables...being greater than a specified threshold. The bivariate risk ...robability refers to the likelihood that various conditions will occur simultaneously hold...

删除了: risk ...robabilities and return periods are given according to the univariate return period formula. The first type is when two variables simultaneously reach a given threshold, which will be defined as the simultaneous risk

删除了: 3

删除了: 4...). The second type is that at least one variable reaches a given threshold, which is defined as the joint risk

删除了: 5

删除了: 6...). The third type is the conditional risk

删除了: 7

删除了: 8...), where whenWhen...one of the variables reaches a given threshold, the other variable also reaches a certain threshold. The calculation ...ormula is expressed

删除了: 223

删除了: 334

删除了: 445

删除了: 556



$$P_1 = P((X > x)|(Y > y)) = \frac{P(X > x, Y > y)}{P(Y > y)} = \frac{1 - P(X \leq x) - P(Y \leq y) + P(X \leq x, Y \leq y)}{1 - P(Y \leq y)}$$

$$= \frac{1 - F_X(x) - F_Y(y) + F_{X,Y}(x, y)}{1 - F_Y(y)}$$

删除了: 667

$$RP_1 = \frac{E_L}{P((X > x)|(Y > y))} = \frac{E_L \cdot (1 - F_Y(y))}{1 - F_X(x) - F_Y(y) + F_{X,Y}(x, y)}$$

删除了: 778

where  $F_X(x)$  and  $F_Y(y)$  are the marginal functions of the univariate  $X$  and  $Y$ , respectively, and  $F_{X,Y}(x, y)$  is the joint distribution function of the two-dimensional variables  $(X, Y)$ .

删除了: distribution

删除了: variables

### 3.3.3 Combined scenario probability

To carry out the tropical cyclone storm surge and wave combination scenario simulation, we classify the SH and SWH into five classes (Table 2) by referring to the *Technical directives for risk assessment and zoning of marine disasters—Part 1: Storm Surge* (MNR, 2019) and *Part 2: Waves* (MNR, 2021).

We calculate the bivariate probabilities for discretized hazard level combination scenarios based on the marginal and copula functions of the storm surge and wave. The formula is as follows:

删除了: Based on the marginal and copula functions of the storm surge and wave, we calculate the bivariate risk probabilities for different hazard level combination scenarios

删除了: calculation

删除了: expressed

删除了: 889

$$P_{\&} = P(x_1 < X \leq x_2, y_1 < Y \leq y_2)$$

$$= P(X \leq x_2, Y \leq y_2) - P(X \leq x_2, Y \leq y_1) - P(X \leq x_1, Y \leq y_2) + P(X \leq x_1, Y \leq y_1)$$

$$= F_{X,Y}(x_2, y_2) - F_{X,Y}(x_2, y_1) - F_{X,Y}(x_1, y_2) + F_{X,Y}(x_1, y_1)$$

删除了: TC

Table 2 Hazard level classification criteria for combined scenarios of tropical cyclone surge height and significant wave height

Hazard level	Surge height (m)	Significant wave height (m)
I	[2.5, +∞)	[14.0, +∞)
II	[2.0, 2.5)	[9.0, 14.0)
III	[1.5, 2.0)	[6.0, 9.0)
IV	[1.0, 1.5)	[4.0, 6.0)
V	[0.0, 1.0)	[0.0, 4.0)

删除了: TC

删除了: L

## 3.4 Design of protection standards for storm surge and wave

### 3.4.1 Probability changes under increased storm surge and wave protection standards

In actual engineering protection design, if the protection standards of SH and SWH are appropriately increased or decreased, it can change the simultaneous bivariate probability  $P_0$ , joint bivariate probability  $P_0$ , and conditional bivariate probability

删除了: Risk

删除了: p

删除了: risk

删除了: risk

删除了: risk

$P_1$ . In this paper, we try to estimate the change value of the bivariate probability by raising the return period of storm surge or wave. The formula is as follows:

$$\begin{aligned} P_{d\cap} &= P((X > x_2) \cap (Y > y)) - P((X > x_1) \cap (Y > y)) \\ &= P(X \leq x_2, Y \leq y) - P(X \leq x_2) - P(X \leq x_1, Y \leq y) + P(X \leq x_1) \\ &= F_{X,Y}(x_2, y) - F_X(x_2) - F_{X,Y}(x_1, y) + F_X(x_1) \end{aligned} \quad (9)$$

$$\begin{aligned} P_{d\cup} &= P((X > x_2) \cup (Y > y)) - P((X > x_1) \cup (Y > y)) = P(X \leq x_1, Y \leq y) - P(X \leq x_2, Y \leq y) \\ &= F_{X,Y}(x_1, y) - F_{X,Y}(x_2, y) \end{aligned} \quad (10)$$

$$\begin{aligned} P_{d1} &= P((X > x_2)|(Y > y)) - P((X > x_1)|(Y > y)) \\ &= \frac{P(X \leq x_2, Y \leq y) - P(X \leq x_2) - P(X \leq x_1, Y \leq y) + P(X \leq x_1)}{1 - P(Y \leq y)} \\ &= \frac{F_{X,Y}(x_2, y) - F_X(x_2) - F_{X,Y}(x_1, y) + F_X(x_1)}{1 - F_Y(y)} \end{aligned} \quad (11)$$

where  $P_{d\cap}$ ,  $P_{d\cup}$ , and  $P_{d1}$  are the changes of the simultaneous probability  $P_{\cap}$ , the joint probability  $P_{\cup}$ , and the conditional probability  $P_1$  after the univariate return period is raised, and  $x_1$  and  $x_2$  are the intensity values of variable  $X$  for different return periods, respectively, where  $x_2 > x_1$ .

### 3.4.2 Design storm surge and wave criteria for joint return period scenarios

The joint probabilities of storm surge and wave scenarios are hard to be directly employed as reference values for engineering protection standards, since the bivariate joint probability and joint return period is a three-dimensional surface, and the intercepted curve under the specified occurrence probability or return period is a curve, not a scalar. For the combined event of extreme surge height and significant wave height, a series of  $(x, y)$  are designed to maximize  $P\{X > x, Y > y\}$  under the given joint return period, to obtain the optimal combined design value. Therefore, we explore the design criteria for the combined storm surge and wave scenarios based on the joint return periods  $RP_{\cup}$  and simultaneous return periods  $RP_{\cap}$ . Under the constraint that the joint return period of surge height and significant wave height is  $K$ , the maximum simultaneous bivariate probability is selected as the objective function. This is the case where the bivariate probability is the maximum considering the correlation of two hazard indicators, and the corresponding simultaneous return period is the smallest, which is the most

删除了: risk

删除了: protection standard

删除了: scenarios

删除了: expressed

删除了: 9910

删除了: 101011

删除了: 111112

删除了: reduced values

删除了: risk

删除了: risk

删除了: risk

删除了: protection standard

删除了: ,

删除了: marginal and

删除了: cannot

删除了: risk

删除了: risk

删除了: disaster-causing factor

删除了: s

appropriate case for prevention (Xu et al., 2022). Therefore, the optimal design criteria for storm surge and wave scenarios are estimated using the non-linear programming method (Bazaraa et al., 2006). The formula is expressed as follows:

Constraint condition:

$$\begin{cases} K = RP_U = \frac{E_L}{P((X > x) \cup (Y > y))} = \frac{E_L}{1 - P(X \leq x, Y \leq y)} = \frac{E_L}{1 - F_{X,Y}(x, y)} \\ x \in (0, 40) \\ y \in (0, 40) \end{cases} \quad (12)$$

Objective function:

$$\max \{P_n\} = \min \{RP_n\} = \min \left\{ \frac{E_L}{P((X > x) \cap (Y > y))} \right\} = \min \left\{ \frac{E_L}{1 - F_X(x) - F_Y(y) + F_{X,Y}(x, y)} \right\} \quad (13)$$

## 4 Results and discussion

### 4.1 Optimal marginal function

Since the different densities and locations of the triangular grids in the storm surge and wave models, we use the storm surge triangular grid nodes as the benchmark and the wave node closest to each storm surge node as the wave simulation result based on the nearest neighbor method. Therefore, a dataset of storm surges and waves with the same number and location of nodes is reconstructed, containing 1665 nodes in the study area.

In this paper, based on the reconstructed storm surge and wave simulation results of historical TC events, we calculate each node's annual extreme values of SH and SWH. Firstly, the time series of the bivariate annual maximum value for all nodes are fitted with five marginal functions, including Gumbel, Weibull, gamma, exponential, and generalized extreme value (GEV). Next, the p-value of the K-S test is used to determine whether the hypothesis that the sample obeys a certain theoretical distribution is rejected. Then, we count the number of nodes passing the K-S test for each function and their percentage of all nodes. Finally, the number of nodes and their percentage of each function being selected as optimal is calculated according to the steps for optimal function selection in Section 3.1 (Table 3).

**Table 3** Frequency and percentage of five functions passing the K-S test and the optimal function for all nodes of SH and SWH

Marginal	Surge height	Significant wave height
----------	--------------	-------------------------

删除了: 121213

删除了: 131314

删除了: y

删除了: network

删除了: model

删除了: differ

删除了: nodes of the storm surge triangular

删除了: network

删除了: use

删除了: the annual extremes of SH and SWH for each node

删除了: Next

删除了: marginal functions by

删除了: distribution

删除了: , and

删除了: fitting effect is judged by the

删除了: it passes the 95% significance level.

删除了: Next

删除了: frequency

删除了: each type of function

删除了: in

删除了: and its percentage of the total number of nodes

<u>function</u>	<u>Frequency</u> <u>of K-S test</u> <u>passed</u>	<u>Percentage</u> <u>of K-S test</u> <u>passed (%)</u>	<u>Frequency</u> <u>of optimal</u> <u>function</u>	<u>Percentage</u> <u>of optimal</u> <u>function (%)</u>	<u>Frequency</u> <u>of K-S test</u> <u>passed</u>	<u>Percentage</u> <u>of K-S test</u> <u>passed (%)</u>	<u>Frequency</u> <u>of optimal</u> <u>function</u>	<u>Percentage</u> <u>of optimal</u> <u>function (%)</u>
<u>Gamma</u>	<u>1508</u>	<u>90.57</u>	<u>183</u>	<u>10.99</u>	<u>1464</u>	<u>87.93</u>	<u>159</u>	<u>9.55</u>
<u>Exponential</u>	<u>1567</u>	<u>94.11</u>	<u>216</u>	<u>12.97</u>	<u>1076</u>	<u>64.62</u>	<u>95</u>	<u>5.71</u>
<u>Gumbel (right)</u>	<u>1615</u>	<u>97.00</u>	<u>350</u>	<u>21.02</u>	<u>1629</u>	<u>97.84</u>	<u>149</u>	<u>8.95</u>
<u>Weibull (max)</u>	<u>1469</u>	<u>88.23</u>	<u>416</u>	<u>24.98</u>	<u>300</u>	<u>18.02</u>	<u>494</u>	<u>29.66</u>
<u>GEV</u>	<u>1665</u>	<u>100.00</u>	<u>500</u>	<u>30.04</u>	<u>1657</u>	<u>99.52</u>	<u>768</u>	<u>46.13</u>

删除了:  
Marginal function

...

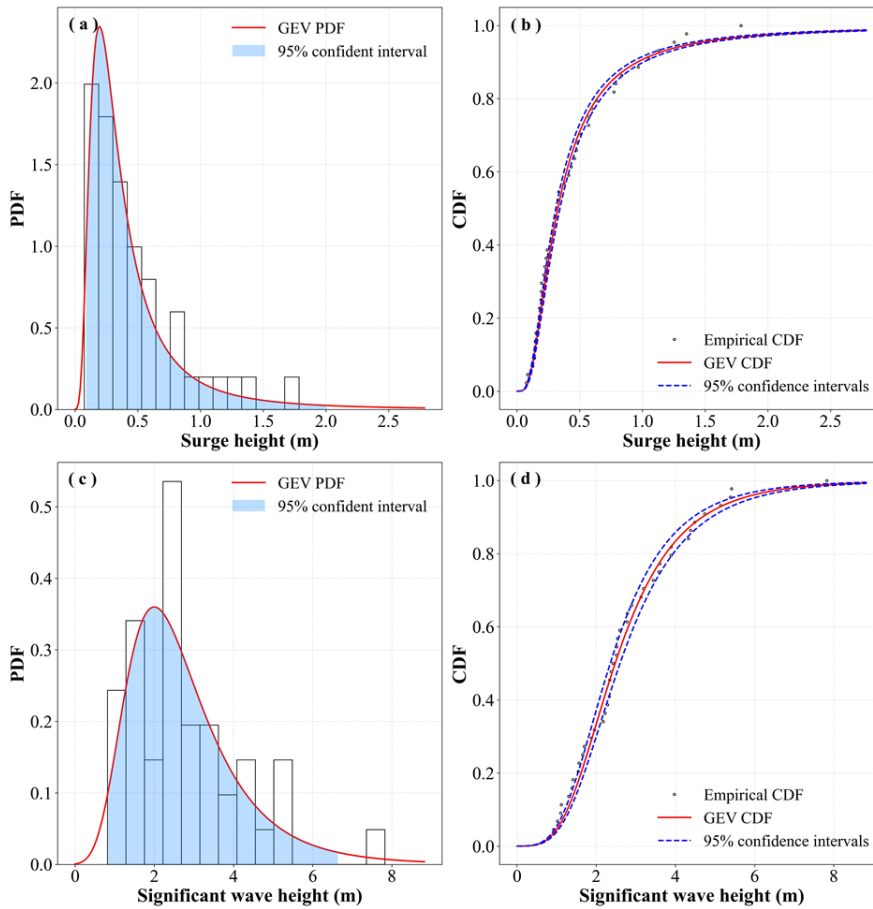


Figure 3: Fitting results of the PDF and CDF of the SH and SWH based on the GEV function (using node (110.5142° E, 20.2768° N) as an example)

Based on the statistical results, it is found that for fitting the SH, the K-S test of the GEV function had the highest no-rejection rate of 100%, and the corresponding optimal ratio was 30.04%, so GEV is set as the optimal marginal function in this study.

删除了: it is determined that the GEV function has the highest K-S test pass rate of 100% for the univariate fitting of SH...

For SWH fitting, the number of nodes [with no rejection in](#) the K-S test [of](#) the GEV function is 1657, accounting for 99.52% of the total number of nodes, [and the corresponding percentage of preferences is also](#) higher than [that of](#) other functions. We apply the GEV function to fit the marginal function of the SH and SWH at all nodes and calculate the PDF, CDF, and RP. Figure 3 shows an example of the PDF and CDF of the SH and SWH for a [given](#) node.

#### 4.2 Distribution of univariate return periods

Based on the univariate return period formula (Eq. [4](#)), the SH and SWH are estimated for six typical return periods of 5a, 10a, 20a, 50a, 100a, and 200a at all nodes. To analyze the [distribution characteristics of the univariate return period in this study area](#), we chose the cubic spline interpolation method to interpolate the intensity values at each node with different return periods into a raster with a resolution of 1 km (Figure 4 and Figure 5).

As shown in Figure 4, the SH shows a significant increasing trend as it approaches the coastline. [The](#) SH along the eastern coast of the Leizhou Peninsula is higher than that in other regions, mainly influenced by factors such as TC landing location, landing direction, and pocket-shaped coastal topography. The [TCs in the northern hemisphere are](#) counterclockwise rotations affected by the deflecting force. Therefore, northeastern Hainan Island is located on the southern coast of the Qiongzhou Strait, and the northeast and northwest winds of TCs affecting the region easily cause seawater accumulation, [a](#) storm surge-prone area. The TC wind fields in the east and south of Hainan Island are [less favorable to water gain than](#) those in the north. Therefore, the offshore surge height on Hainan Island shows a [distribution pattern of high](#) in the northeast and [low](#) in the southeast. [As the return period increases, SH offers varying degrees of growth in each region, and regional differences are more pronounced, with a significant area of development in southeastern Hainan Island, which may be related to the region's location on the edge of the continental shelf and high variability in seafloor topography.](#)

删除了: passing

删除了: for

删除了: which is

删除了: fitting

删除了: 2

删除了: study area's

删除了: distribution characteristics

删除了: In general, the

删除了: N

删除了: H

删除了: TCs

删除了: which is

删除了: not as favorable to water gain as

删除了: high

删除了: a

删除了: distribution

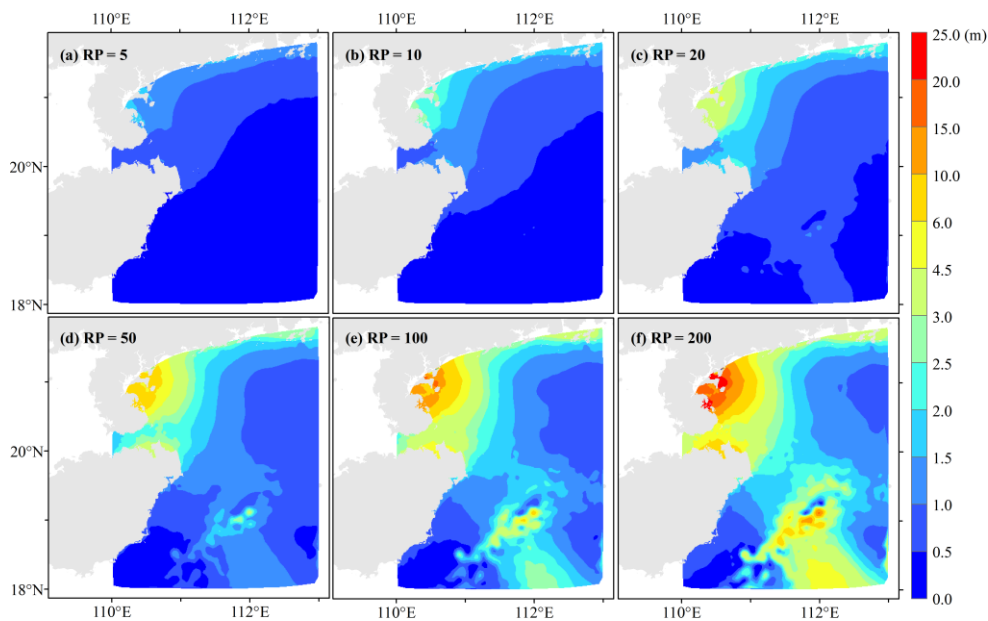


Figure 4: Spatial distribution of surge heights of tropical cyclones for six typical return periods

570 As shown in Figure 5, the SWH near the shore is generally smaller than that in the open sea, and there is a significant decreasing trend in SWH as it gets closer to the coastline. This finding is mainly attributed to the shallow shore depth, island obstruction, wave breaking, and seabed friction attenuation. Among them, the SWH in the eastern Leizhou Peninsula is lower than that of other seas, which is mainly influenced by the curved depressed coastline and the topography of the shore section. The SWHs are high in the east and south of Hainan Island, where there is a more significant gradient due to the wave-breaking effect and dissipation caused by the region's dramatic change in water depth. The SWH in the north of Hainan Island is low, and the shift from sea to land is relatively slow.

删除了: deep

删除了: offers

删除了: approaches

删除了: and is

删除了: and concave

删除了: is high

删除了: because of

删除了: dramatic change in water depth in the region

删除了: , so there is a more significant gradient

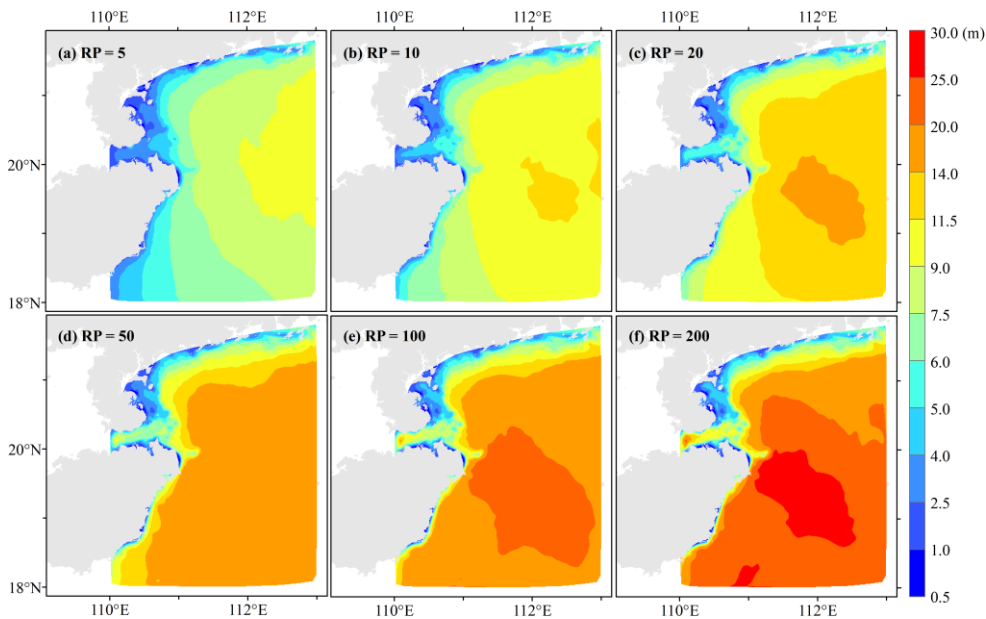


Figure 5: Spatial distribution of significant wave heights of tropical cyclones for six typical return periods

### 4.3 Optimal copula function

The optimal GEV function is utilized as the marginal function for the TC storm surges and waves, based on which three copula functions are applied to the bivariate joint fitting of 1665 nodes. The function parameters are fitted by the maximum likelihood method, and the K-S test is used to determine whether the [hypothesis that the sample obeys a certain functional distribution is rejected](#). Next, we count the number of nodes that pass the K-S test for the three types of copula functions and their percentage of the total number of nodes (Table 4). The statistical results show that the number of nodes passing the K-S test for the Gumbel copula function is 1603, accounting for 96.28% of all nodes, so it is used as the optimal copula function in this study. The Gumbel copula function is applied to the bivariate joint fitting of SH and SWH for all nodes, and the PDF and CDF are calculated.

删除了: fit passes the 95% significance level

删除了: Figure 6 shows an example of the PDF and CDF of a node's optimal copula function for SH and SWH.



Table 4 Frequency and percentage of three copula functions passing the K-S test for all nodes of surge height and significant wave height of tropical cyclones

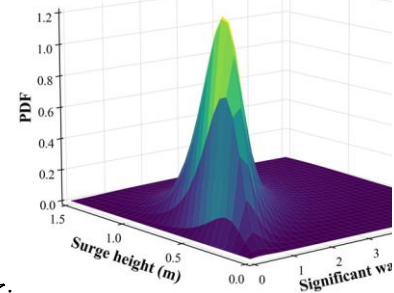
Copula function	Frequency	Percentage (%)
Clayton	486	29.19
Frank	1398	83.96
Gumbel	1603	96.28

#### 4.4 Distribution of bivariate probabilities and return periods

Based on the optimal marginal function and copula function, we calculate  $RP_{\cap}$ ,  $RP_{\cup}$ , and  $RP_{|}$  of SHs and SWHs. In addition, based on the formula of bivariate probability (Eq. 2 and Eq. 4),  $P_{\cap}$  and  $P_{\cup}$  of SH and SWH are calculated for all nodes with four typical combinations of return periods of 10a, 20a, 50a, and 100a. To analyze the distribution characteristics,  $P_{\cap}$  and  $P_{\cup}$  for different combinations of return periods at each node are interpolated into a raster with a resolution of 1 km using the cubic spline interpolation method (Figure 6 and Figure 7).

The simultaneous bivariate probability  $P_{\cap}$  gradually decreases as the return period of SH or SWH increases (Figure 6).

Overall, the closer to the coastline, the higher  $P_{\cap}$ .  $P_{\cap}$  is greatest when the return period of SH and SWH is 10a, which is higher than 0.05.  $P_{\cap}$  is the smallest for SH and SWH of 100a, which is generally lower than 0.009.



删除了:

Figure 6: Fitting results of PDF and CDF for two-dimensional joint tropical cyclone surge height and significant wave height based on the Gumbel copula function (using the node (110.5142° E, 20.2768° N) as an example)

删除了: risk

删除了: distribution

删除了: When the intensity values of the two disaster-causing factors are equivalent,  $RP_{\cap}$  is greater than  $RP_{\cup}$ , which indicates that  $P_{\cap}$  is smaller than  $P_{\cup}$ . Figure 7 shows an example of  $RP_{\cap}$  and  $RP_{\cup}$  for the SH and SWH at a node based on the optimal copula function. ...

删除了: B

删除了: risk

删除了: 3

删除了: 5

删除了: Figure 6Figure 6Figure 8

删除了: Figure 7Figure 7Figure 9

删除了: Bivariate

删除了: Figure 6Figure 6Figure 8

删除了: In general

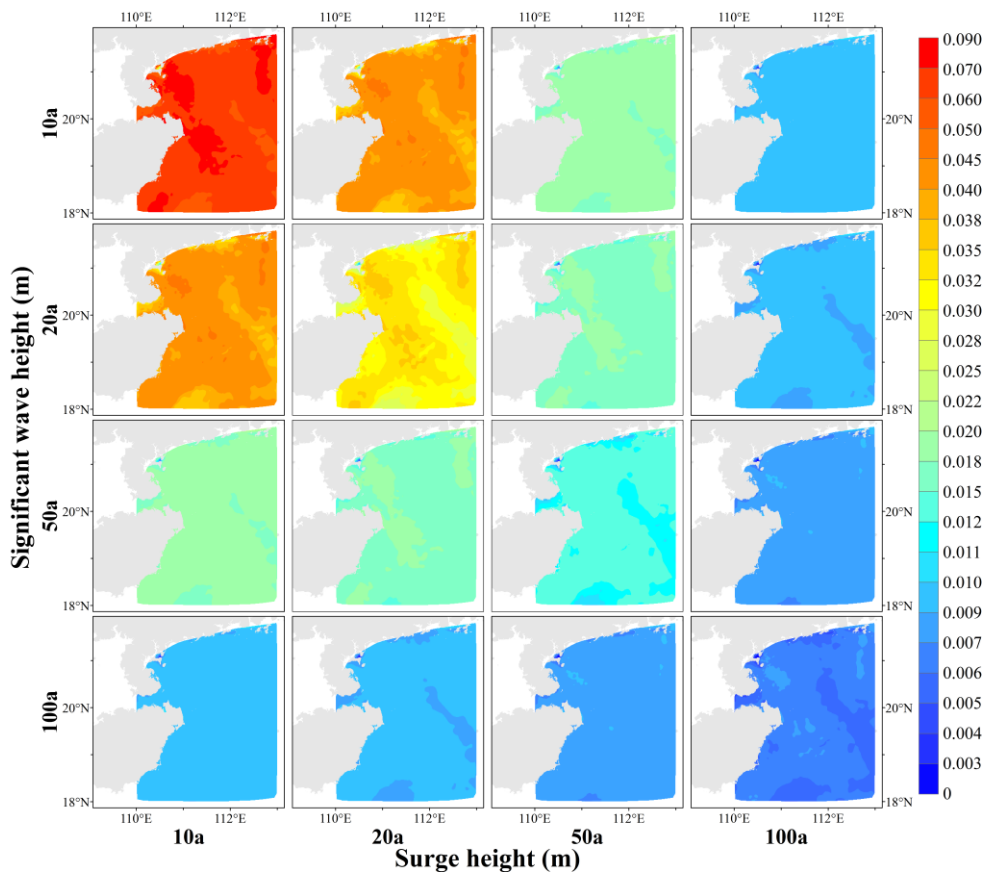


Figure 6: Simultaneous probabilities of combined scenarios with four typical return periods for surge height and significant wave heights of tropical cyclones

The joint bivariate probability  $P_U$  of SH and SWH is higher than  $P_{\cap}$ , and it gradually decreases with an increasing return period of the two hazard indicators (Figure 7). Overall, the closer to the coastline, the higher  $P_U$ .  $P_U$  is highest when the return period of SH and SWH is 10a, which is greater than 0.13 overall.  $P_U$  is smallest when the return period for SH and SWH is 100a, which is less than 0.015. When the return period of SH or SWH is 50a or 100a, the regional variation in  $P_U$  are

删除了: disaster-causing factors

删除了: Figure 7Figure 7Figure 9

删除了: are

删除了: of

删除了: are

删除了: differences

relatively small.

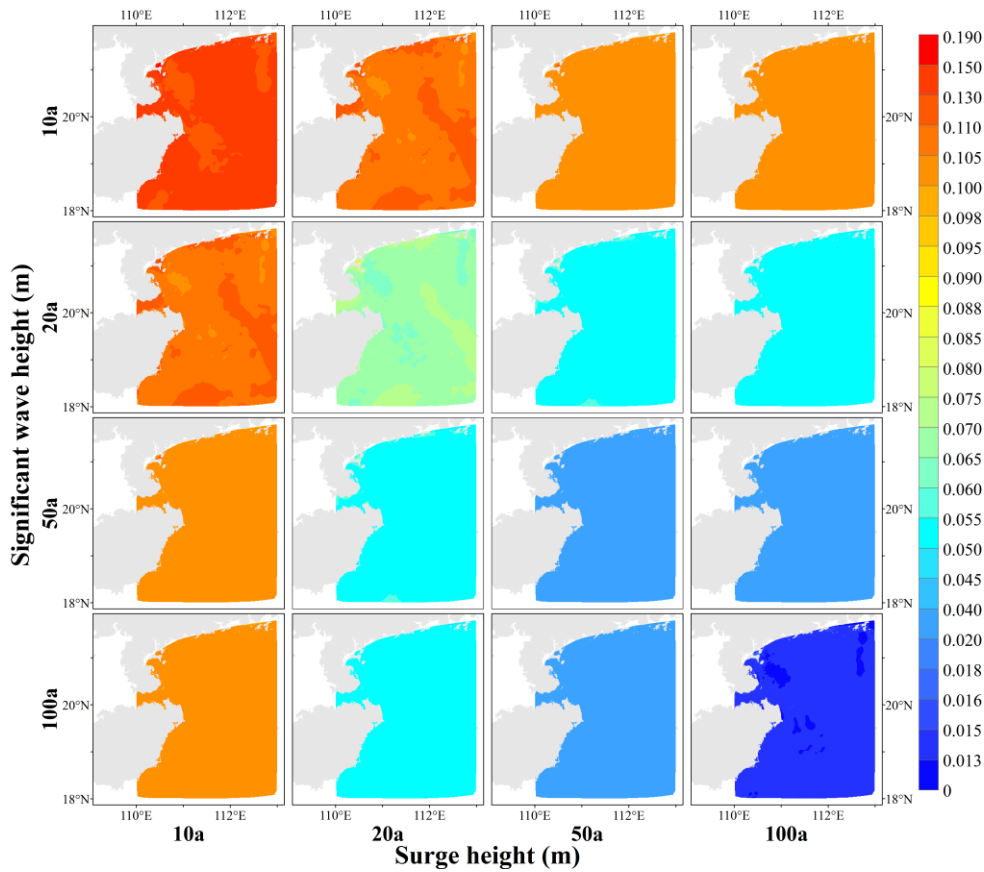


Figure 7: Joint probabilities of combined scenarios with four typical return periods for surge height and significant wave heights of tropical cyclones

660 Based on the formula of conditional bivariate probability  $P_{ij}$  (Eq. 6), we calculate  $P_{ij}$  for all nodal univariate<sub>s</sub> with different return periods for the other variable in four return periods, interpolate them into 1 km raster data using cubic spline interpolation. According to the formula, the calculation results are consistent when the positions of the variables are swapped. Therefore,

删除了: 7  
 删除了: nodes  
 删除了: and

only  $P_i$  for the four return periods of SH in different wave return periods are shown in this paper (Figure 8). When the SWH is a specific return period,  $P_i$  gradually decreases as the return period of the SH increases. Under the condition that the return period of SWH is 10a,  $P_i$  for SH with a return period of 10a are concentrated between 0.55 and 0.75, and  $P_i$  is generally less than 0.08 if the return period for SH is 100a. When the return periods of SWHs and SHs are equivalent, the  $P_i$  is concentrated between 0.55 and 0.75.

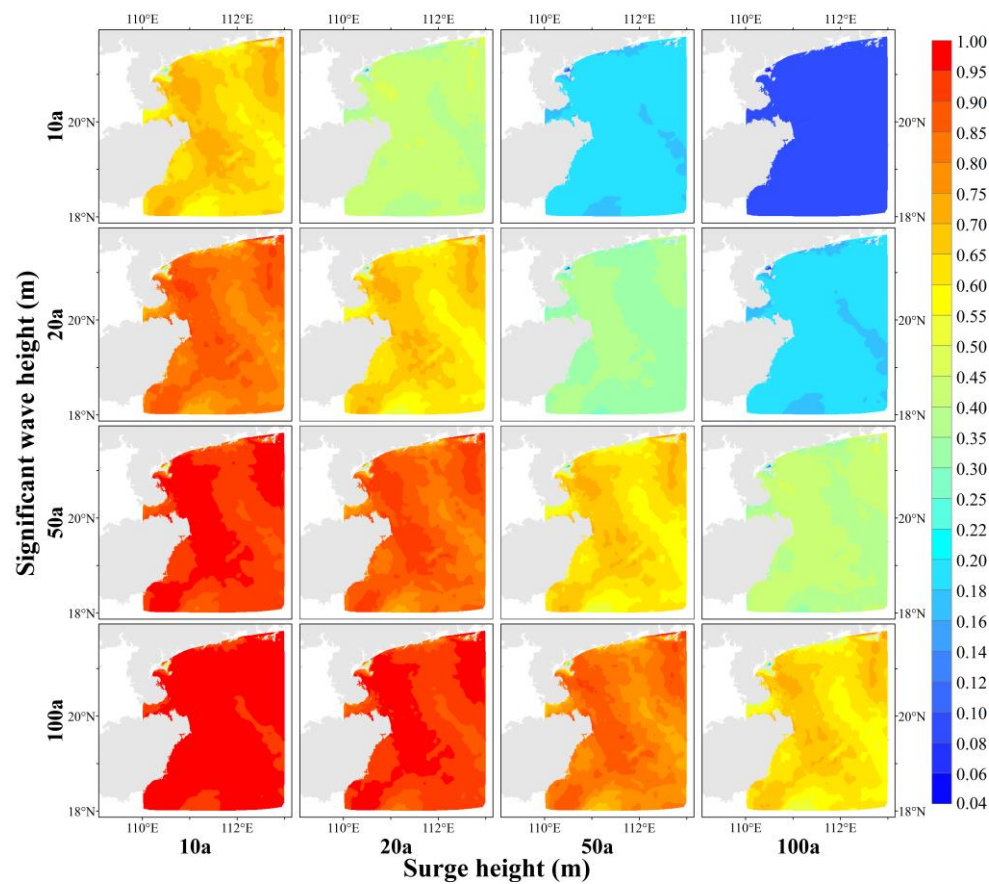


Figure 8: Conditional probabilities of bivariate for different return periods of tropical cyclone significant wave heights

删除了: Figure 8Figure 8Figure 10

删除了: bivariate

删除了: bivariate

删除了: bivariate

删除了: of are

680 According to the classification criteria of [the hazard indicators](#), (Table 2), SH and SWH are divided into five classes. We calculate [the combined scenario probability](#)  $P_{s\&}$  based on Eq. [8](#) for all nodes with different combinations of SH and SWH for a total of 25 scenarios and interpolate them into 1 km raster data using the cubic spline interpolation method ([Figure 9](#)).

[Regarding](#) the vertical variation pattern, [when](#) the SH [hazard level is determined](#), as the SWH [hazard level](#) increases, the high-value area of the combined scenario probability gradually moves away from the coastline, and the scope of the nearshore low-value area gradually expands. This result is consistent with the geographic distribution pattern that the SWH is low [in](#) nearshore and high [in](#) offshore. In the horizontal variation [pattern](#), when the SWH [hazard level](#) is determined, as the SH [hazard level](#) increases, the range of low-value areas for the combined scenario probabilities expand, and the low-value area's left boundary gradually approaches [the](#) coastline. This result is consistent with the geographic distribution of SHs being high nearshore and low offshore. Overall, the maximum value of the probability for each combined scenario tends to decrease as the [hazard level](#) of SH or SWH increases. The larger SH and SWH are concentrated in the eastern Leizhou Peninsula at a certain distance [from](#) [the coast](#), [with other areas](#) less likely to occur.

685

删除了: disaster-causing factors

删除了: two-dimensional

删除了:  $U$

删除了: 9

删除了: Figure 9Figure 9Figure 11

删除了: risk

删除了: law

删除了: risk

删除了: s

删除了: risk

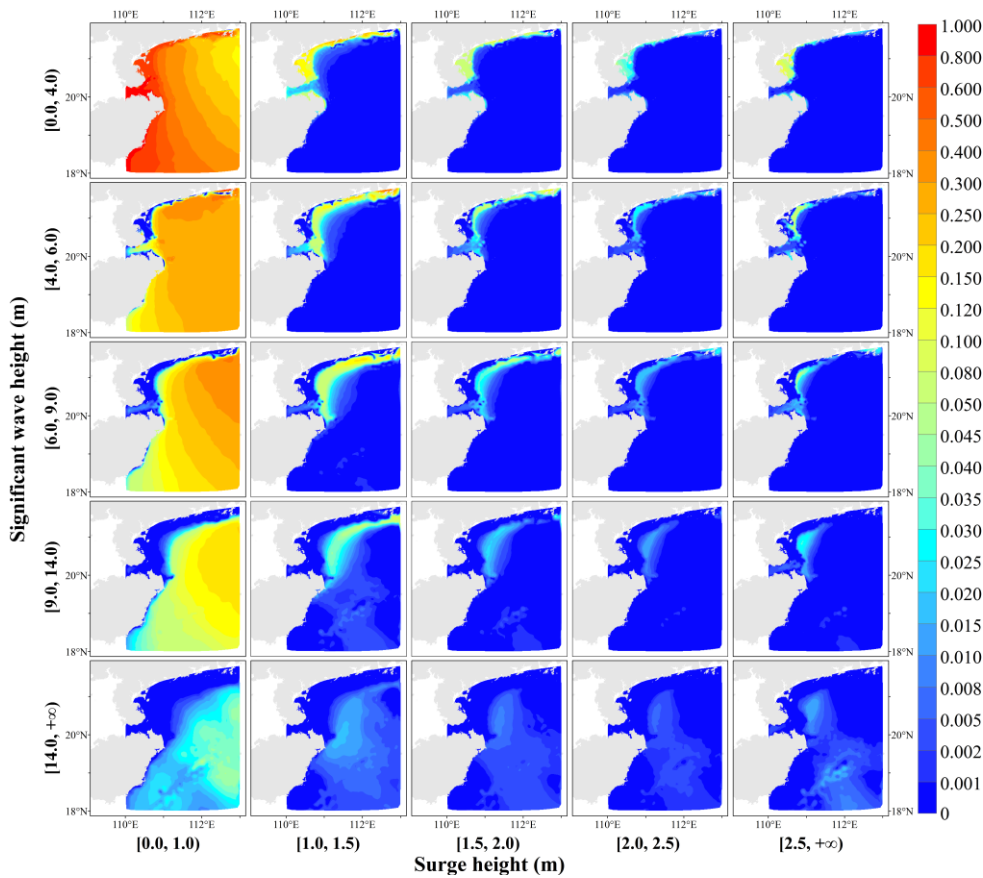


Figure 9: Probabilities of combined scenarios with different levels of surge height and significant wave height for tropical cyclones

Based on the calculated  $P_{\cap}$ ,  $P_U$ ,  $P_I$ , and  $P_{\&}$  with different return periods, Markov chain Monte Carlo (MCMC) and other methods can be further applied to generate random samples for [quantitatively assessing](#) TC storm surges and waves. On the other hand, we can explore the effect of [varying the intensity values of](#) SH and SWH on the bivariate joint [probabilities](#) and apply it to the [engineering design](#) criteria.

删除了: the quantitative assessment of

删除了: changes in

删除了: risk

删除了: design of

删除了: protection

#### 4.5 Design storm surge and wave criteria

In the design of the engineering fortification criteria, if one hazard indicator is dominant, upgrading the return period for the other variable can effectively change bivariate  $P_{\cap}$  and  $P_{\cup}$  when the conditions for their return period fortification criteria are determined. In this paper, we calculate the change in probability based on Eq. 9, Eq. 10, and Eq. 11 to determine the shift in the probability that remains constant when the positions of the two hazard indicators are switched. Therefore, we calculate the change values in  $P_{\cap}$ ,  $P_{\cup}$ , and  $P_{\Delta}$  for all nodes when the design return period criterion for a given variable is increased from 5a, 10a, 20a, and 50a to 10a, 20a, 50a, and 100a, respectively. And the data are interpolated into 1 km raster data using the cubic spline interpolation method (Figure 10, Figure 11, and Figure 12).

Figure 10 shows the distribution of the reduction values of bivariate  $P_{\cap}$  for the scenario with elevated univariate return period protection criteria. As the return period protection criteria of one variable increase, the decline in  $P_{\cap}$  gradually decreases as the return period of the other variable's protection standard increases. Its reduction is concentrated between 0 and 0.035. When the return period protection standard of one variable is fixed, as the protection criteria of another variable are gradually increased, the decline of  $P_{\cap}$  rises to a certain level and then tends to decrease. When the return period of one variable is 10a or 20a, the decline in  $P_{\cap}$  increases when the protection standard of another variable is raised. If the design criteria increase from 50a to 100a, the change value of  $P_{\cap}$  decreases.

删除了: disaster-causing factor

删除了: is

删除了: is increased under

删除了: that

删除了: its

删除了: standard is

删除了: , which can effectively change bivariate  $P_{\cap}$  and  $P_{\cup}$

删除了: risk

删除了: 10

删除了: 11

删除了: 12

删除了: that

删除了: risk

删除了: the same

删除了: disaster-causing factors

删除了: of

删除了: are calculated

删除了: of SH and SWH for one variable with return periods of 10a, 20a, 50a, and 100a protection criteria when the design return period criteria for the other variable are raised

删除了: Figure 10Figure 10Figure 12

删除了: Figure 11Figure 11Figure 13

删除了: Figure 12Figure 12Figure 14

删除了: Figure 10Figure 10Figure 12

删除了: reduced

删除了: In general, as

删除了: decrease

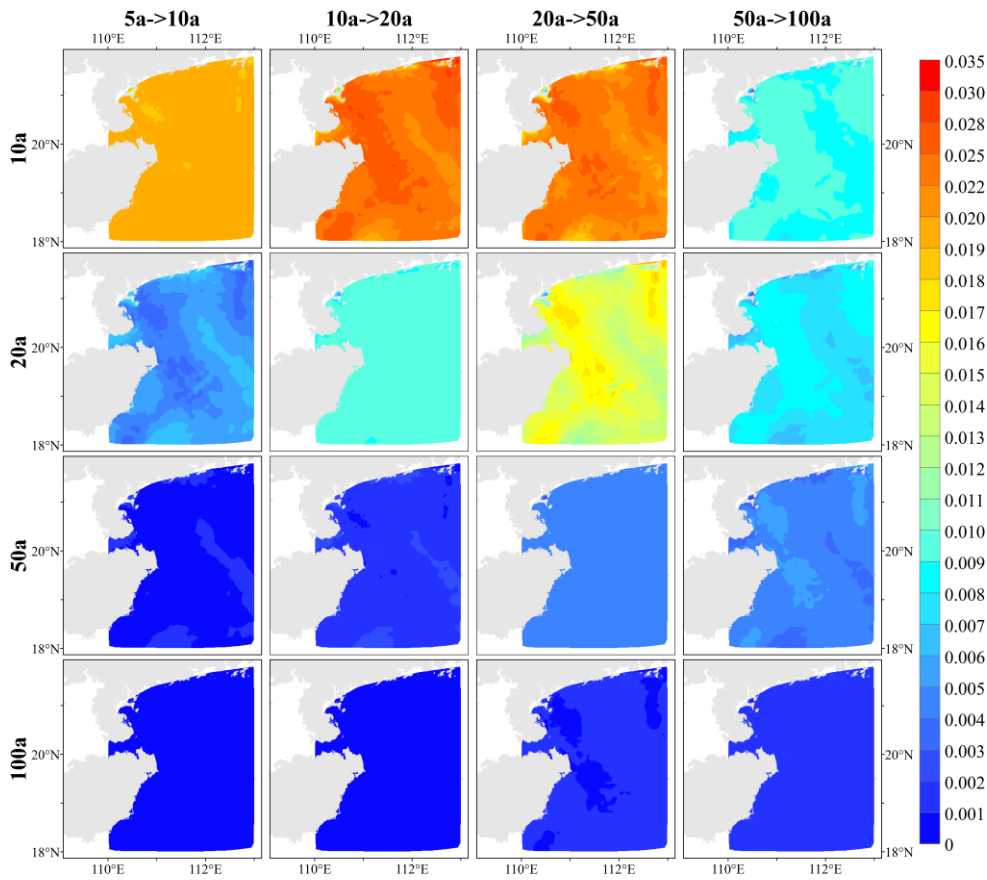


Figure 10: Difference in the simultaneous probability of tropical cyclone surge height and significant wave height for scenarios with elevated return period protection standards

Figure 11 shows the distribution of the reduced values for bivariate  $P_U$  when the protection criteria for the univariate return period is increased. Among them,  $P_U$  decreases more than  $P_D$ , and the reduced value of  $P_U$  varies from 0 to 0.105. As the return period protection standard for one variable gradually increases,  $P_U$  slowly decreases after the protection criteria for the

删除了: Figure 11Figure 11Figure 13

删除了: with

删除了: elevated

删除了: protection criteria

删除了: In general



other variable increase. When the return period protection criterion for one variable is fixed, the decline in  $P_U$  gradually

765 decreases as the design criteria for the other variable are increased.

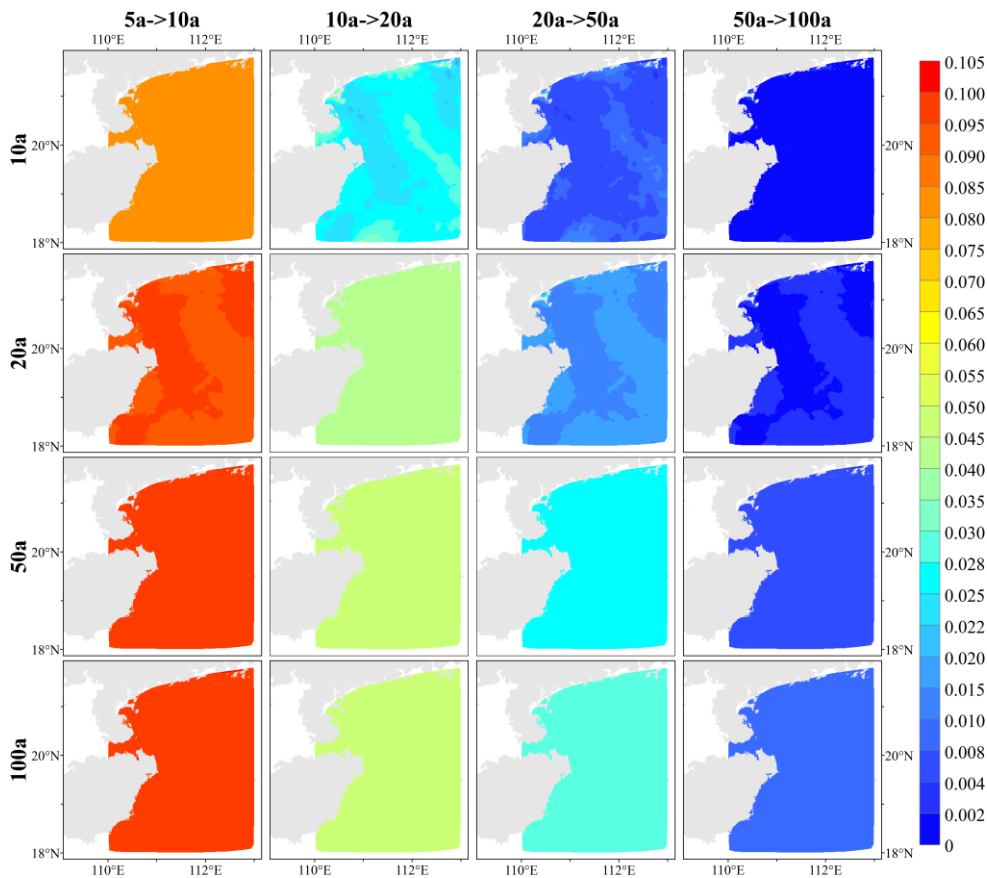


Figure 11: Difference in joint probability of tropical cyclone surge height and significant wave height for scenarios with elevated return period protection standards

770 Figure 12 shows the distribution of the reduced values of bivariate  $P_I$  for the scenario of raising the univariate return period protection criteria. As the return period for one variable increases, there is a decreasing trend in the decrease in  $P_I$  after the

design criteria for the other variable are raised.  $P_1$  has a more significant decrease than  $P_{\Gamma}$  and  $P_U$ , and the decreasing value of  $P_1$  varies from 0 to 0.45. When the protection level of one variable is fixed and low, the reduction in  $P_1$  will tend to decrease after the design criteria of another variable are raised to a certain level. When the protection standard for one variable is 10a or 20a, the decrease in bivariate  $P_1$  tends to increase when the design criterion for the other variable's return period is raised, but the decrease in  $P_1$  is slightly reduced when the design criterion of the other variable is increased from 50a to 100a. If the protection level of one variable is high, the decrease in  $P_1$  after the protection standard of the other variable is raised always tends to increase.

775

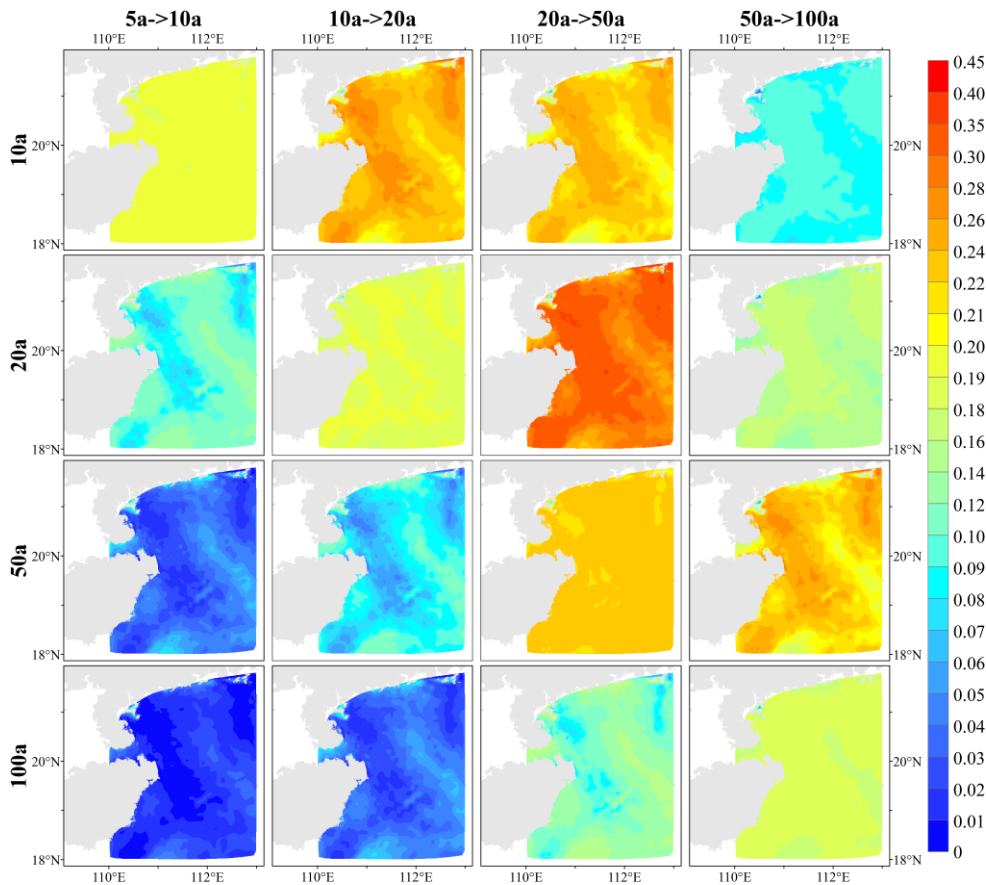


Figure 12: Differences in the conditional probability of tropical cyclone surge height and significant wave height for scenarios with elevated return period protection standards

In the engineering design criteria, the appropriate design surge height and significant wave height are set according to the bivariate  $RP_U$  and  $RP_D$ , the estimation method is shown in Section 3.4.2. In this paper, the design values of SH and SWH for six  $RP_U$  for all nodes are calculated based on the above method and interpolated to 1 km raster data by the cubic spline interpolation method (Figure 13 and Figure 14). The design criteria for SH and SWH show an apparent increasing trend as the

删除了: design of

删除了: standards

删除了: based on

删除了: of SH and SWH to set the appropriate reference value of the protection standards

删除了: Figure 13Figure 13Figure 15

删除了: Figure 14Figure 14Figure 16

删除了: In general, with an increase in the return period, the

删除了: of

return period increases, with the high-value area for SH constantly concentrated east of the Leizhou Peninsula, and the high-value area for SWH concentrated in the east of Hainan Island.

When  $RP_U$  is 5a, the design criteria of SH are between 1.5 m and 2.5 m in the eastern coastal area of the Leizhou Peninsula and fall below 0.5 m in the southeastern coastal region of Hainan Island. As the return period increases, the design surge height gradually increases, and when  $RP_U$  is 200 a, the design surge height in the eastern coastal area of the Leizhou Peninsula is generally higher than 3.0 m. The design surge height in the northeast coastal area of Hainan Island is mainly between 3.0 m and 15.0 m, while that in the southeast coastal region of Hainan Island is between 0.5 m and 2.0 m, which is lower than that in the northeast.

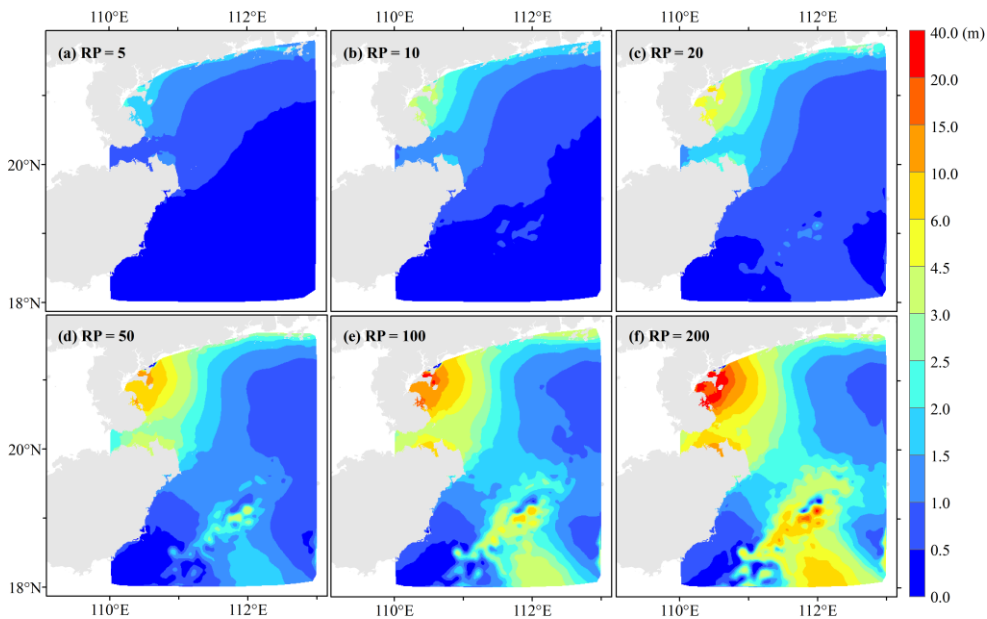


Figure 13: Design surge heights for six typical joint return period scenarios

When  $RP_U$  is 5a, the design criteria of SWH in the coastal areas of the Leizhou Peninsula and Hainan Island are less than 2.5 m overall. The further from the coastline, the protection standard gradually increases. As the return period increases, the design

删除了: in which

删除了: of

删除了: is

删除了: ,

删除了: of

删除了: is

删除了: ern sea area

删除了: SH

删除了: standard

删除了: SH

删除了: standard

删除了: SH

删除了: standard

删除了: mainly

820 criteria of SWH gradually increase, and the growth is more evident than that of SH. When  $RP_U$  is 200 a, SWH along the coast  
of the Leizhou Peninsula is generally less than 6.0 m, while the [design SWH](#) along the Qiongzhou Strait and southeastern  
Hainan Island is relatively high.

删除了: design standard

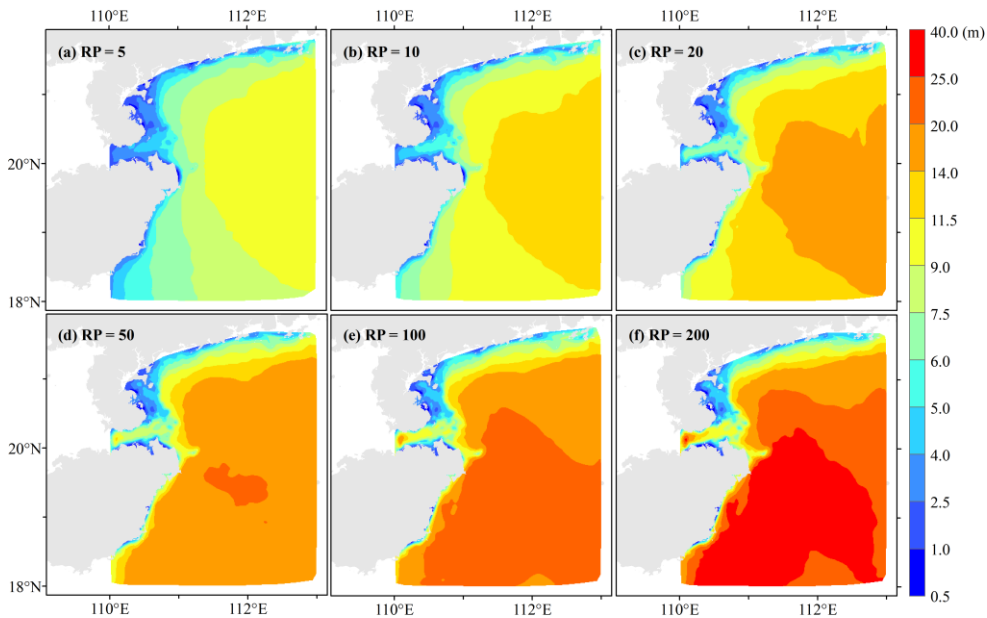


Figure 14: Design significant wave heights for six typical joint return period scenarios

## 825 5 Conclusions

[In this study, we aimed to estimate joint probability analysis on storm surge and waves using Copula functions on a large dataset from a wide area, and determine their respective design standards as scalar values of SWH and SH. Our main conclusions are as follows:](#)

1) The GEV function [is the most suitable for](#) the probability distribution characteristics of the annual extremes of tropical cyclone SH and SWH for all nodes in the study area. The Gumbel copula function is [appropriate](#) as a bivariate joint distribution

删除了: is the best fit for

删除了: suitable

830

function for all nodes in the study area.

2) The hazard of a single indicator can be characterized by the univariate intensity values with different return periods, which the optimal marginal function can estimate. Our findings show that the SH exhibits a significant increasing trend closer to the coastline, while SWH is higher farther from the shoreline across different return periods. However, we also observe apparent spatial heterogeneity in the distribution, influenced by factors such as the shoreline shape, coastal and submarine topography, and deflection forces.

3) Bivariate probabilities are utilized in this study to assess the integrated hazard of multiple indicators, including  $P_{\cap}$ ,  $P_{\cup}$ ,  $P_{\bar{\cap}}$ , and  $P_{\bar{\cup}}$ , which effectively compensates for the deficiency of disregarding the correlation among variables in univariate hazard assessment. These four probabilities can visually describe the occurrence probability for different combinations of scenarios; the more significant the probability is, the higher the hazard. Overall,  $P_{\bar{\cap}}$  is the largest,  $P_{\cup}$  is the second largest, and  $P_{\cap}$  is the smallest, while  $P_{\bar{\cup}}$  is influenced by the classification of single hazard indicators. When one variable is constant,  $P_{\cap}$ ,  $P_{\cup}$ , and  $P_{\bar{\cap}}$  tend to decrease as the return period of the other variable increases.

4) In actual design criteria, the bivariate  $P_{\cap}$ ,  $P_{\cup}$ , and  $P_{\bar{\cap}}$  can be reduced by appropriately increasing the design surge height and significant wave height. When the return period protection standard of one variable is fixed, as the design criteria of another variable gradually increase, the decline in  $P_{\cap}$  and  $P_{\bar{\cap}}$  rises to a certain level and then tends to decrease, but the decline in  $P_{\cup}$  gradually decreases. Therefore, the development of appropriate design surge heights and significant wave heights can be effective in reducing hazard impacts, which allows coastal areas to cope with a high bivariate probability. To obtain the specific scaler values of the two hazards as design criteria, in this study, the method for estimating the minimum return periods of SH and SWH was implemented, given their estimated joint probability distribution as a constraint.

Although this study provides helpful insights into joint probability analysis of storm surges and waves using Copula functions, there are several limitations that need to be addressed in future research. One limitation is the absence of water level rise caused by storm surges in the numerical modeling of waves, which may introduce errors in the simulation of SWHs in intermediate and shallow water. In addition, exploring the contribution of other indicators, such as long-term sea level rise as environmental hazards, can further improve the accuracy of risk assessment.

删除了: in this study area

删除了: disaster-causing factor... can be characterized by the univariate intensity values with different return periods, which the optimal marginal function can estimate estimated by the optimal marginal distribution function... Our findings show thatIn general,...the SH exhibits shows ... significant increasing trend closer to the coastline, while and ...WH is higher farther from the shoreline across in...different return periods. However, we also observethe distribution has...apparent spatial heterogeneity in the distribution, influenced by factors such as the shoreline shape, coastal topography...nd,

删除了: Due to the data dimensionality, it is difficult to estimate the exact value of the univariate intensity for a given return period. Therefore, ...ivariate risk ...robabilities are utilized in this study to assess the integrated hazard of multiple indicatorsjoint hazard of multiple disaster-causing

删除了: Based on the occurrence probability for different SH and SWH scenarios, many random samples can be generated

删除了: -

删除了: segmentation of the causal factors

删除了: the design of ...ctual engineering ...esign fortification ...riteriastandards

删除了: criteria of SH or SWH can be appropriately improved to reduce bivariate  $P_{\cap}$ ,  $P_{\cup}$ , and  $P_{\bar{\cap}}$ .

删除了: As the return period protection standard of one variable increases, the decline in  $P_{\cap}$  and  $P_{\bar{\cap}}$  tends to

删除了: impact...of disasters can be effectively reduced by setting ...ppropriate return period ...esign standards for

删除了: Since the changing trends of  $P_{\cap}$  and  $P_{\cup}$  are the opposite. These two indicators can be used as constraintsand

删除了: In this paper, the two most commonly employed indicators of SH and SWH are selected for TC storm surge

**Author contributions.** FWH and ZHX conceived the research framework and developed the methodology. ZHX was responsible for the code compilation, data analysis, graphic visualization, and first draft writing. FWH managed the implementation of research activities and revised the manuscript. CM participated in the data collection of this study. All authors discussed the results and contributed to the final version of the paper.

**Competing interests.** The authors declare that they have no conflict of interest.

**Acknowledgments.** This work was mainly supported by the National Key Research and Development Program of China (grant nos. 2017YFA0604903 and 2018YFC1508803) and the Key Special Project for Introduced Talents Team of Southern Marine Science and Engineering Guangdong Laboratory (Guangzhou) (grant no. GML2019ZD0601). We [are grateful to](#) Xing Liu of the Ocean University of China for providing the simulation data of storm surges and waves for historical tropical cyclone events.

**Financial support.** This research has been supported by the National Key Research and Development Program of China (grant nos. 2017YFA0604903 and 2018YFC1508803), and the Key Special Project for Introduced Talents Team of Southern Marine Science and Engineering Guangdong Laboratory (Guangzhou) (grant no. GML2019ZD0601).

## References

- Bazaraa, M. S., Sherali, H. D., and Shetty, C. M.: Nonlinear programming: Theory and algorithms, Third Edit., John Wiley & Sons, Ltd, Hoboken, New Jersey, 872 pp., <https://doi.org/https://doi.org/10.1002/0471787779>, 2006.
- Bilskie1, M. V., Hagen, S. C., Medeiros, S. C., Cox, A. T., Salisbury, M., and Coggin, D.: Data and numerical analysis of astronomic tides, wind-waves, and hurricane storm surge along the northern Gulf of Mexico, *J. Geophys. Res. Ocean.*, 121, 3625–3658, <https://doi.org/10.1002/2015JC011400>, 2016.
- Bomers, A., Schielen, R. M. J., and Hulscher, S. J. M. H.: Consequences of dike breaches and dike overflow in a bifurcating river system, *Nat. Hazards*, 97, 309–334, <https://doi.org/10.1007/s11069-019-03643-y>, 2019.
- Brown, J. M.: A case study of combined wave and water levels under storm conditions using WAM and SWAN in a shallow water application, *Ocean Model.*, 35, 215–229, <https://doi.org/10.1016/j.ocemod.2010.07.009>, 2010.
- Chen, L. and Guo, S.: Copulas and its application in hydrology and water resources, First Edit., Springer Singapore, Singapore, 290 pp., <https://doi.org/10.1007/978-981-13-0574-0>, 2019.
- Chen, Y. and Yu, X.: Sensitivity of storm wave modeling to wind stress evaluation methods, *J. Adv. Model. Earth Syst.*, 9, 893–907, <https://doi.org/10.1002/2016MS000850>, 2017.

删除了: thank

- 1035 Chen, Y., Li, J., Pan, S., Gan, M., Pan, Y., Xie, D., and Clee, S.: Joint probability analysis of extreme wave heights and surges along China's coasts, *Ocean Eng.*, 177, 97–107, <https://doi.org/10.1016/j.oceaneng.2018.12.010>, 2019.
- Corbella, S. and Stretch, D. D.: Simulating a multivariate sea storm using Archimedean copulas, *Coast. Eng.*, 76, 68–78, <https://doi.org/10.1016/j.coastaleng.2013.01.011>, 2013.
- Galiatsatou, P. and Prinos, P.: Joint probability analysis of extreme wave heights and storm surges in the Aegean Sea in a changing climate, *E3S Web Conf.*, 7, 1–12, <https://doi.org/10.1051/e3sconf/20160702002>, 2016.
- 1040 Hsu, C. H., Olivera, F., and Irish, J. L.: A hurricane surge risk assessment framework using the joint probability method and surge response functions, *Nat. Hazards*, 91, S7–S28, <https://doi.org/10.1007/s11069-017-3108-8>, 2018.
- Huang, Y., Weisberg, R. H., Zheng, L., and Zijlema, M.: Gulf of Mexico hurricane wave simulations using SWAN: Bulk formula-based drag coefficient sensitivity for Hurricane Ike, *J. Geophys. Res. Ocean.*, 118, 3916–3938, <https://doi.org/10.1002/jgrc.20283>, 2013.
- 1045 Hughes, S. A. and Nadal, N. C.: Laboratory study of combined wave overtopping and storm surge overflow of a levee, *Coast. Eng.*, 56, 244–259, <https://doi.org/10.1016/j.coastaleng.2008.09.005>, 2009.
- Jang, J. H. and Chang, T. H.: Flood risk estimation under the compound influence of rainfall and tide, *J. Hydrol.*, 606, 127446, <https://doi.org/10.1016/j.jhydrol.2022.127446>, 2022.
- 1050 Kimf, K. O., Yuk, J., Leen, H. S., and Choi, B. H.: Typhoon Morakot induced waves and surges with an integrally coupled tide-surge-wave finite element model, *J. Coast. Res.*, 2, 1122–1126, <https://doi.org/10.2112/S175-225.1>, 2016.
- Lee, D. Y. and Jun, K. C.: Estimation of design wave height for the waters around the Korean Peninsula, *Ocean Sci. J.*, 41, 245–254, <https://doi.org/10.1007/BF03020628>, 2006.
- Lee, T., Modarres, R., and Ouarda, T. B. M. J.: Data-based analysis of bivariate copula tail dependence for drought duration and severity, *Hydrol. Process.*, 27, 1454–1463, <https://doi.org/10.1002/hyp.9233>, 2013.
- 1055 Li, J., Fang, W., Zhang, X., Cao, S., Yang, X., Liu, X., and Sun, J.: Similar tropical cyclone retrieval method for rapid potential storm surge and wave disaster loss assessment based on multiple hazard indicators, *Mar. Sci.*, 40, 49–60, <https://doi.org/10.11759/hyxx20151104001>, 2016.
- Li, L., Pan, Y., Amini, F., and Kuang, C.: Full scale study of combined wave and surge overtopping of a levee with RCC strengthening system, *Ocean Eng.*, 54, 70–86, <https://doi.org/10.1016/j.oceaneng.2012.07.021>, 2012.
- 1060 Lin, N., Emanuel, K. A., Smith, J. A., and Vanmarcke, E.: Risk assessment of hurricane storm surge for New York City, *J. Geophys. Res. Atmos.*, 115, 1–11, <https://doi.org/10.1029/2009JD013630>, 2010.
- Liu, X., Jiang, W., Yang, B., and Baugh, J.: Numerical study on factors influencing typhoon-induced storm surge distribution in Zhanjiang Harbor, *Estuar. Coast. Shelf Sci.*, 215, 39–51, <https://doi.org/10.1016/j.ecss.2018.09.019>, 2018.
- 1065 Lu, X., Yu, H., Ying, M., Zhao, B., Zhang, S., Lin, L., Bai, L., and Wan, R.: Western North Pacific Tropical Cyclone Database Created by the China Meteorological Administration, *Adv. Atmos. Sci.*, 38, 690–699, <https://doi.org/10.1007/s00376-020-0211-7>, 2021.
- Marcos, M., Rohmer, J., Vousdoukas, M. I., Mentaschi, L., Le Cozannet, G., and Amores, A.: Increased extreme coastal water levels due to the combined action of storm surges and wind waves, *Geophys. Res. Lett.*, 46, 4356–4364, <https://doi.org/10.1029/2019GL082599>, 2019.
- 1070 MNR: Technical directives for risk assessment and zoning of marine disaster--Part 1: Storm surge, 2019.



- MNR: Technical directives for risk assessment and zoning of marine disaster--Part 2: Wave, Beijing, 1–30 pp., 2021.
- Morellato, D. and Benoit, M.: Constitution of a numerical wave data-base along the French Mediterranean coasts through hindcast simulations over 1979–2008, *Chart*, 1–8, <https://doi.org/10.13140/2.1.1794.3049>, 2010.
- 1075 Muraleedharan, G., Rao, A. D., Kurup, P. G., Nair, N. U., and Sinha, M.: Modified Weibull distribution for maximum and significant wave height simulation and prediction, *Coast. Eng.*, 54, 630–638, <https://doi.org/10.1016/j.coastaleng.2007.05.001>, 2007.
- Nelsen, R. B.: An introduction to copulas, Second Edi., Springer Science+Business Media, New York, 1–656 pp., 2006.
- 1080 Niedoroda, A. W., Resio, D. T., Toro, G. R., Divoky, D., Das, H. S., and Reed, C. W.: Analysis of the coastal Mississippi storm surge hazard, *Ocean Eng.*, 37, 82–90, <https://doi.org/10.1016/j.oceaneng.2009.08.019>, 2010.
- Pan, Y., Li, L., Amini, F., and Kuang, C.: Full-scale HPTRM-strengthened levee testing under combined wave and surge overtopping conditions: Overtopping hydraulics, shear stress, and erosion analysis, *J. Coast. Res.*, 29, 182–200, <https://doi.org/10.2112/JCOASTRES-D-12-00010.1>, 2013.
- 1085 Pan, Y., Zhang, Z., Yuan, S., Zhou, Z., and Chen, Y.: An overview of research on combined wave and surge overtopping on levees, *Adv. Sci. Technol. Water Resour.*, 39, 90–94, <https://doi.org/10.3880/j.issn.1006-7647.2019.01.015>, 2019.
- Papadimitriou, A. G., Chondros, M. K., Metallinos, A. S., Memos, C. D., and Tsoukala, V. K.: Simulating wave transmission in the lee of a breakwater in spectral models due to overtopping, *Appl. Math. Model.*, 88, 743–757, <https://doi.org/10.1016/j.apm.2020.06.061>, 2020.
- 1090 Perk, L., van Rijn, L., Koudstaal, K., and Fordeyn, J.: A rational method for the design of sand dike/dune systems at sheltered sites; Wadden Sea Coast of Texel, the Netherlands, *J. Mar. Sci. Eng.*, 7, 1–25, <https://doi.org/10.3390/jmse7090324>, 2019.
- Petroliagkis, T. I., Voukouvalas, E., Disperati, J., and Bidlot, J.: Joint probabilities of storm surge, significant wave height and river discharge components of coastal flooding events. Utilising statistical dependence methodologies and techniques, Publications Office of the European Union, Luxembourg, 79 pp., <https://doi.org/10.2788/677778>, 2016.
- 1095 Rao, X., Li, L., Amini, F., and Tang, H.: Numerical study of combined wave and surge overtopping over RCC strengthened levee systems using the smoothed particle hydrodynamics method, *Ocean Eng.*, 54, 101–109, <https://doi.org/10.1016/j.oceaneng.2012.06.024>, 2012.
- Serinaldi, F.: Dismissing return periods!, *Stoch. Environ. Res. Risk Assess.*, 29, 1179–1189, <https://doi.org/10.1007/s00477-014-0916-1>, 2015.
- 1100 Shi, X., Han, Z., Fang, J., Tan, J., Guo, Z., and Sun, Z.: Assessment and zonation of storm surge hazards in the coastal areas of China, *Nat. Hazards*, 100, 39–48, <https://doi.org/10.1007/s11069-019-03793-z>, 2020.
- Sklar, A.: Random variables, joint distribution functions, and copulas, *Kybernetika*, 9, 449–460, 1973.
- Teena, N. V., Sanil Kumar, V., Sudheesh, K., and Sajeev, R.: Statistical analysis on extreme wave height, *Nat. Hazards*, 64, 223–236, <https://doi.org/10.1007/s11069-012-0229-y>, 2012.
- 1105 Trepanier, J. C., Needham, H. F., Elsner, J. B., and Jagger, T. H.: Combining surge and wind risk from hurricanes using a copula model: An example from Galveston, Texas, *Prof. Geogr.*, 67, 52–61, <https://doi.org/10.1080/00330124.2013.866437>, 2015.
- Wahl, T., Mudersbach, C., and Jensen, J.: Assessing the hydrodynamic boundary conditions for risk analyses in coastal areas: A multivariate statistical approach based on Copula functions, *Nat. Hazards Earth Syst. Sci.*, 12, 495–510,

<https://doi.org/10.5194/nhess-12-495-2012>, 2012.

1110 Wahl, T., Jain, S., Bender, J., Meyers, S. D., and Luther, M. E.: Increasing risk of compound flooding from storm surge and rainfall for major US cities, *Nat. Clim. Chang.*, 5, 1093–1097, <https://doi.org/10.1038/nclimate2736>, 2015.

Xie, D. mei, Zou, Q. ping, and Cannon, J. W.: Application of SWAN+ADCIRC to tide-surge and wave simulation in Gulf of Maine during Patriot’s Day storm, *Water Sci. Eng.*, 9, 33–41, <https://doi.org/10.1016/j.wse.2016.02.003>, 2016.

1115 Xu, H., Tan, J., Li, M., and Wang, J.: Compound flood risk of rainfall and storm surge in coastal cities as assessed by copula formal, *J. Nat. Disasters*, 31, 40–48, <https://doi.org/10.13577/j.jnd.2022.0104>, 2022.

Zhang, B. and Wang, S.: Probabilistic characterization of extreme storm surges induced by tropical cyclones, *J. Geophys. Res. Atmos.*, 126, 1–22, <https://doi.org/10.1029/2020JD033557>, 2021.